Tribol Lett (2015) 58:15
DOI 10.1007/s11249-015-0480-y

METHODS PAPER

A Dichromatic Interference Intensity Modulation Approach to Measurement of Lubricating Film Thickness

Hai Chao Liu · Feng Guo · Liang Guo · Pat Lam Wong

Received: 22 September 2014 / Accepted: 15 January 2015 / Published online: 11 March 2015

Abstract The study aims to extend the measurement range of dichromatic interferometry in lubricating film thickness measurement. Subtraction of two sets of interference fringes, which are produced by dichromatic (red and green) lights, gives a modulated signal of intensity against film thickness. The measuring range without wavelength ambiguity is limited to the first half-cycle of the beat wave in the modulated signal. Theoretical and experimental analyses of the modulated interference intensity variation against film thickness were conducted. The differences in the pattern of the modulated interference intensity were obtained in the first three half-cycles of the beat wave. Based on that, a robust dichromatic interference intensity modulation approach for lubricating film measurement was derived and its measuring range without wavelength ambiguity was successfully extended to the magnitude equivalent to three half-cycles of the beat wave. To test the feasibility and credibility of this approach, the film thickness in elastohydrodynamic and hydrodynamic lubricated contacts was measured. The results were well correlated with the classical theory. Using red and green lasers with wavelength of 653 and 532 nm, respectively, the measurement range can be extended to 4 μm.

H. C. Liu · F. Guo (✉)
School of Mechanical Engineering, Qingdao Technological University, 11 Fushun Road, Qingdao 266033, China
e-mail: mefguo@163.com

L. Guo · P. L. Wong
Department of Mechanical and Biomedical Engineering, City University of Hong Kong, 83 Tat Chee Avenue, Kowloon, Hong Kong, China

Keywords Dichromatic interferometry · Intensity modulation · Multi-beam interferometry · Lubricating film thickness

1 Introduction

Optical interferometry has been widely used for determining the thickness of transparent films. Its application in lubrication studies can be traced back to the early twentieth century when it was realized that the wavelength of visible lights was at the same order of magnitude as the thickness of lubricating films. For example, Hardy and Hardy [1] made use of white light interference colors to estimate the thickness of fluid films between two convex glass surfaces. Later in the 1960s, Kirk [2] successfully measured the hydrodynamic lubrication film thickness between two crossed perspex cylinders. Cameron et al. [3–7] applied optical interferometry technique to the study of elastohydrodynamic lubrication (EHL) and obtained significant results, such as the first ever image of the classical horseshoe EHL film shape including the outlet constriction and the side lobes. The optical EHL test setup of Cameron et al. adopted a steel ball on a transparent (glass or sapphire) disk configuration, which is still widely used nowadays in the tribology community. Details about the optical EHL interferometry, for example, the use of a Cr film as the beam splitter for high contrast fringes and a spacer layer for extending the minimum measurement limit, were well-documented [3–7]. For conventional optical lubrication systems, monochromatic or chromatic (white) light sources are employed. Monochromatic light provides excellent fringe visibility even when the film thickness is large. With any constructive or destructive interference fringes, the film thickness can be estimated, respectively, by the following equations.

$$2nh + \frac{\varphi_0}{2\pi}\lambda = N\lambda \tag{1}$$

$$2nh + \frac{\varphi_0}{2\pi}\lambda = \left(N - \frac{1}{2}\right)\lambda \tag{2}$$

where n is the refractive index of the lubricant, h is the film thickness, φ_0 is the initial phase of the measurement system, λ is the light wavelength and N is the fringe order. Within the range of actual film thickness up to $\lambda/(2n)$, the fringe order N must be equal to 1 if there exists any constructive or destructive fringe. When the film is thick, the order of an interference fringe is not known by the fringe itself. Due to the unknown N, the film thickness cannot be determined exclusively and may have different values according to Eqs. (1) and (2). The differences between these possible values are an integral number of $\lambda/2$. This problem is generally known as wavelength ambiguity. Tedious fringe order counting cannot be avoided. In other words, the absolute film thickness cannot be inferred from a single interferogram without knowing the order of any fringe. On the other hand, since white light interferogram contains more color information, such as the number of wavelengths and differences in color fringe sequences, film thickness can be determined without relying on known fringe orders. Hence, it is desirable for lubricating film thickness measurement. However, due to color saturation when film thickness increases, the maximum detectable film thickness is usually not larger than 1 μm. As a compromise between the monochromatic interferometry and white light interferometry, dichromatic interferometry has also been used, in which red and green lights obtained by a filter are usually employed [8–10].

With the advent of affordable digital image hardware in the 1990s, the optical interferometry has been greatly improved, in particular, for measuring very thin lubricating films at nanoscale resolution. These new approaches fall essentially into three categories, that is, spectrum analysis, computerized colorimetry and interference intensity digitization. The approach of spectrum analysis was proposed by Johnston et al. [11], in which white light interference is employed and the wavelength of constructive interference is accurately determined by a spectrometer to get the film thickness. With a spacer layer of SiO_2, they claimed that lubricant film in the range of 1–500 nm can be determined with an accuracy of ±0.5 nm. More recently, the capability of colorimetry technique has been enhanced [12, 13], for example, more accurately identifying the wavelength of constructive interference and obtaining the optical properties of EHL films. Computerized colorimetry enables interferograms to be directly scanned and analyzed by using color CCDs and analyzers. Any color changes can be more precisely recognized. Therefore, the film thickness can be obtained with high resolution and 3-D reconstruction of the film shape is readily executed. Using the concept of color space, different measurement systems are designed, for example, the HSI approach [14], the CIELab method [15] and the RGB scheme [16]. The maximum detectable film thickness of the aforementioned digital colorimetric techniques is generally around 1 μm. Cann et al. [17] proposed a spacer layer imaging method (SLIM) that combines the spacer layer approach and digital colorimetric analyses for ultrathin lubricant film measurement with the range of 0–150 nm at a resolution of 5 nm. Hartl et al. [18] also reported a thin film colorimetric interferometry with nanoscale resolution. Just like other calibration-based methods, the colorimetry technique relies largely on calibration and deviations in the calibration lookup table may lead to significant errors. In monochromatic interferometry, the use of digitized interference intensity enables the film thickness measurement not only to be restricted to the locations of the brightest/darkest fringes (where constructive/destructive interferences occur) as shown in Eqs. (1) and (2), but also to other locations with an intensity value in between. Hence, pseudo-continuous measurement of film thickness can be achieved. Film thickness measurement based on interference intensity can realize high resolution, for example, the relative optical interference intensity technique by Luo et al. [19], and the multi-beam intensity-based approach by Guo and Wong [20]. Nevertheless, to interpret film thickness from a measured interference intensity without wavelength ambiguity is only limited to the measurement range of no larger than $\lambda/(4n)$.

In fact, the thickness of lubricating films is not always at nanoscale, for example, a ball-on-disk contact can present thick film with thickness of several micrometers [6, 21] when the lubrication regime changes from elastohydrodynamic to hydrodynamic lubrication. The typical thickness of hydrodynamic lubricating films is at micrometer scale [22]. When a lubricated contact is running under steady conditions and a full thick lubricating film is developed, the fringes of zero or first order may not appear in the interferogram. Moreover, for running under non-steady conditions, the film thickness varies rapidly in a short time interval and it is difficult to get hold of the absolute fringe order. Therefore, an optical interferometry system with no wavelength ambiguity is valuable.

For length or height measurements, two-wavelength (or heterodyne) interferometry has been proposed and widely used. In this approach, two light beams of different wavelengths are used to generate interference, and the resultant intensity–film thickness variation is signified by a modulating signal or a beat wave with an equivalent wavelength, which is much larger than the individual wavelengths. It thus enlarges the measurement range without wavelength ambiguity [23, 24]. However, due to the dynamic nature of lubrication tests, the typical two-wavelength interferometry system that obtains the two interferograms of an exact area successively with two light sources cannot be directly implemented. Recently, we have applied the dichromatic interferometry technique to the measurement of hydrodynamic lubricating film thickness up to approximately two microns under running conditions [25]. The main aim of this paper is to develop an efficient dichromatic interference intensity modulation (DIIM) approach for lubricating film measurement in a large measurement range without wavelength ambiguity, through conducting theoretical and experimental analyses of the modulated signal produced by the dichromatic light source.

2 Principles of the Dichromatic Interference Intensity Modulation Approach (DIIM)

In the interferometric measurement of lubricating films, a large wavelength means a wide measurement range with no wavelength ambiguity. In this proposed DIIM approach, a dichromatic light generates two sets of interference fringes of different wavelengths (or frequencies). Linear superposition of the two interferograms generates an intensity modulation, which consists of a carrier signal and a modulating signal (also referred to as a beat wave). The beat wave has a large equivalent wavelength that facilitates a wide measurement range without wavelength ambiguity encountered in monochromatic interference.

2.1 DIIM with Two-Beam Interference Theory

When a dichromatic light is incident normally to a contact of a ball or a slider on a glass disk, the interference intensity can be written based on two-beam interferometry as,

$$I_i = \cos(4nh\pi/\lambda_i + \varphi_0), \quad i = r, g \tag{3}$$

where subscripts r and g represent the red and green components of the light source, respectively. It is assumed that the effect of wavelength λ on the refractive index of the lubricant n is negligible. By subtraction of the green and red interference intensity in Eq. (3), a modulated interference intensity I_{m} can be obtained as,

$$\begin{aligned} I_{\mathrm{m}} &= I_{\mathrm{g}} - I_{\mathrm{r}} \\ &= -2\sin\left(2nh\pi\frac{\lambda_{\mathrm{r}} - \lambda_{\mathrm{g}}}{\lambda_{\mathrm{r}}\lambda_{\mathrm{g}}}\right)\sin\left(2nh\pi\frac{\lambda_{\mathrm{r}} + \lambda_{\mathrm{g}}}{\lambda_{\mathrm{r}}\lambda_{\mathrm{g}}} + \varphi_0\right) \\ &= -W_2 \cdot W_1 \end{aligned} \tag{4}$$

where

$$W_1 = \sin\left(2nh\pi\frac{\lambda_{\mathrm{r}} + \lambda_{\mathrm{g}}}{\lambda_{\mathrm{r}}\lambda_{\mathrm{g}}} + \varphi_0\right) \tag{5}$$

and

$$W_2 = 2\sin\left(2nh\pi\frac{\lambda_{\mathrm{r}} - \lambda_{\mathrm{g}}}{\lambda_{\mathrm{r}}\lambda_{\mathrm{g}}}\right) \tag{6}$$

W_1 is known as the carrier signal with a smaller wavelength than those of the individual components λ_{r} and λ_{g}, and W_2 is the modulating signal or beat wave with an equivalent wavelength, $\lambda_{\mathrm{eq}} = \lambda_{\mathrm{r}}\lambda_{\mathrm{g}}/(\lambda_{\mathrm{r}} - \lambda_{\mathrm{g}})$, which is much larger than the wavelengths of the red and green components. For $\lambda_{\mathrm{g}} = 532$ nm and $\lambda_{\mathrm{r}} = 653$ nm, the equivalent wavelength is 2,871 nm. Figure 1 shows an example of the intensity modulation (taking $\varphi_0 = 0$, $n = 1.0$). In fact, this two-wavelength interference strategy, which makes use of the equivalent wavelength λ_{eq} and the phase changes of the two wavelengths to extend the measurement range, has been used to measure surface height [23]. However, the scheme cannot be employed directly due to the dynamic nature of the lubrication tests, and therefore an alternative approach must be found. The modulated interference intensity I_{m} varies with the film thickness showing local intensity extremes (the maxima and minima) of different magnitudes, as shown in Fig. 1. The film thickness can be, theoretically, determined exclusively at theses discrete extremes within a thickness range of $\lambda_{\mathrm{eq}}/2$. However, with noises in the measurement, there may be uncertainties in distinguishing between two adjacent local maxima (or minima) when their difference in intensity magnitude is small, for example, those around the normalized intensity of $I_{\mathrm{m}} = 2$. The most favorable local extremes for film thickness determination are those close to $I_{\mathrm{m}} = 0$. It is better to include one of the points of $I_{\mathrm{m}} = 0$ in the interferogram. A film thickness range larger than $\lambda_{\mathrm{eq}}/2$ is thus preferred. Once the film thickness at one local extreme in an interferogram is obtained, the film thickness at other locations can be determined.

2.2 DIIM with Multi-beam Interference Theory

For a typical optical lubrication system that is either a steel ball or steel slider on a partially Cr-coated glass disk, its optical characteristics are complex due to the high reflectivity of the lubricant/steel interface and the light absorption nature of steel and chromium. The interferogram is thus result of multi-beam interference [6, 12, 20] and the variation of intensity with film thickness deviates from the cosine distribution in Eq. (3). As shown schematically in Fig. 2, a typical optical EHL contact resembles a four-layer optical system. The layers are glass, chromium, lubricant

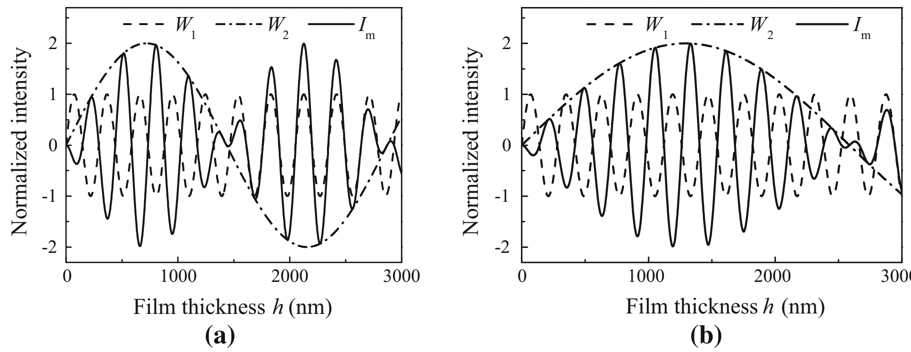

Fig. 1 Illustration of signals W_1, W_2 and I_m in DIIM. **a** $\lambda_g = 532$ nm and $\lambda_r = 653$ nm. **b** $\lambda_g = 532$ nm, $\lambda_r = 593$ nm

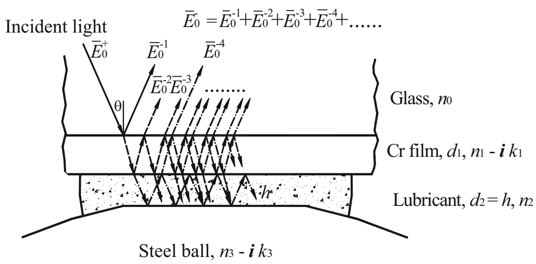

Fig. 2 Multi-beam interference in lubricant film thickness measurement

and steel, and symbolized as media 0–3 accordingly. The chromium film is coated on the glass surface as a beam splitter.

$\bar{E}_0^+$ stands for the electric vector of incident light. $\bar{E}_0^{-m}(m = 1, 2,\ldots)$ denotes the electric vectors generating the interference. The subscript 0 represents the medium number (0: glass) in which the light is traveling. The minus or plus in the superscript represents the propagation direction. m is the vector component number. With the exception of the first one, $\bar{E}_0^{-1}$, which is directly reflected from the Cr/glass interface, all the others are transmitted from layers below. The resultant interference intensity I can be expressed by

$$I = \left|\bar{E}_0^-\right|^2 = \left|\bar{E}_0^{-1} + \bar{E}_0^{-2} + \bar{E}_0^{-3} + \bar{E}_0^{-4} + \cdots\right|^2 = \left|\sum_{m=0}^{\infty} \bar{E}_0^{-m}\right|^2 \quad (7)$$

The detailed numerical scheme of I calculation can be found in [20] and is not repeated here. In the calculations, the wavelength dependence of the refractive indices of the media has been taken into consideration [26, 27]. In two-beam interferometry, only $\bar{E}_0^{-1}$ and $\bar{E}_0^{-4}$ are considered and the variation of intensity and film thickness is a function of cosine.

In the calculation of numerical interferograms, the color tristimulus R, G, B are expressed by

$$C = \int_\lambda S(\lambda) I_h(\lambda) f_C(\lambda) d\lambda, \quad C = R, G, B \quad (8)$$

where $S(\lambda)$ is the spectral density of the incident light and $I(\lambda)$ is the reflectivity from the lubricated contact at wavelength λ, which can be calculated by Eq. (7). $f_R(\lambda)$, $f_G(\lambda)$ and $f_B(\lambda)$ are the spectral sensitivity of the 3CCD sensor.

A computer code has been written to calculate numerical interferograms of a ball-on-disk contact. Figure 3 gives a direct comparison of the simulated and experimental interference images of a steel ball of diameter 25.4 mm in dry contact with a Cr-coated glass plate under a load of 2 N. A dichromatic red and green light with wavelengths of 653 and 532 nm was used, respectively. The CCD spectral sensitivity was extracted from the data sheet of SONY-ICX204AL. Figure 3 shows that the numerical calculation has good visual agreement with the experiment. Figure 4 shows the calculated R and G intensities along with the measured data in the radial direction. The theoretical and experimental results show satisfactory agreement in the initial phase shift and interference intensity distribution. Furthermore, nearly the same normalized intensity at zero film thickness for the two wavelengths validates the assumption of weak dependence of initial phase on the wavelength.

Figure 5 gives the modulated intensity I_m calculated by the multi-beam interference model in Fig. 2. The profile of W_2 acquires a skewed sinusoidal form and deviates from the two-beam interference intensity model as expressed in Eq. (6). Figure 6 presents the modulated intensity curves calculated based on a green light with a constant wavelength of 532 nm and red lights with various wavelengths of 593, 632 and 653 nm. When the magnitude of the wavelength of the red light gets closer to that of the green light, the modulating signal W_2 presents a longer equivalent wavelength, and the number of local extremes increases and differences between them become smaller. From the numerical results, the equivalent wavelength of W_2 can still be calculated by $\lambda_{eq} = \lambda_r\lambda_g/(\lambda_r - \lambda_g)$.

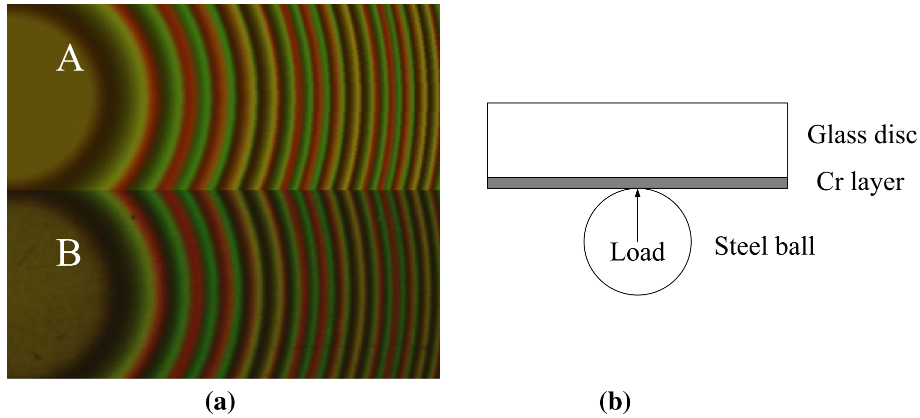

Fig. 3 Simulated and measured interference images of a dry ball-on-disk contact: *A* simulated image; *B* experimental image (ball diameter: 25.4 mm, load: 2 N, $\lambda_g = 532$ nm, $\lambda_r = 653$ nm, $h_{Cr} = 8$ nm). **a** Interference images. **b** ball-on-disk contact

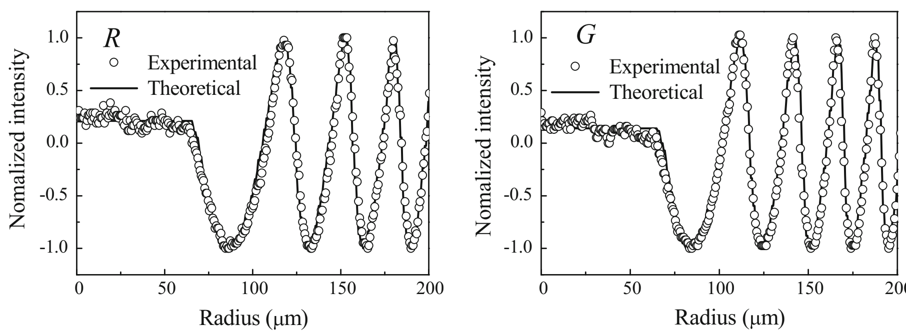

Fig. 4 *R* and *G* intensity components of interference along the radial direction of the ball-on-disk contact in Fig. 3

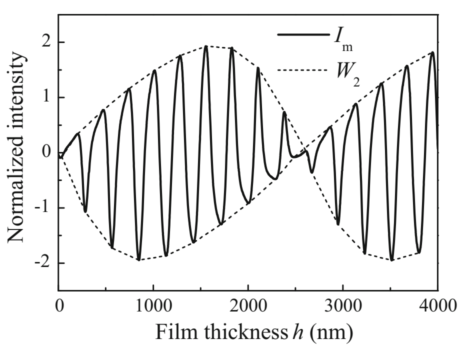

Fig. 5 Calculated interference intensity modulation ($I_m = I_g - I_r$) by multi-beam interference in an optical lubricating film measurement system ($\lambda_g = 532$ nm, $\lambda_r = 593$ nm, $h_{Cr} = 8$ nm)

In an optical lubricating film measurement, dichromatic lights are usually obtained with filters [4, 8–10] and a wide bandwidth of the light source generates low contrast of fringes leading to a low measurement range. In the calculation in Fig. 7, three bandwidths of 1, 10 and 40 nm are used with central wavelengths of 532 and 653 nm for the green and red components, respectively. The optical film thickness range is from 0 to 4,500 nm. It can be seen that for the bandwidths of 1 and 10 nm, the fringes are sharp for the whole film thickness range. However, for the bandwidth of 40 nm, blurred fringes appear and their visibility becomes poor when the film thickness is larger than 1.0 μm. In fact the bandwidth of the common dichromatic filter is close to this value. In the present study, a red–green laser light source was used for achieving clear fringes at high film thickness.

Calculations with different refractive indices of media (air and oil) were also carried out, and the results are shown in Fig. 8 in which the horizontal coordinate is given by optical film thickness *nh*. Figure 8 shows that within the film thickness equivalent to λ_{eq} of W_2, the number of local extremes is the same for the two media. However, the envelope of the modulated intensity, that is the profile of W_2, is different. The W_2 of $n = 1.0$ demonstrates more deviation from a sinusoidal distribution.

Cr film thickness plays an important role in the quality of interferograms. Figure 9 gives the modulated intensity under different Cr layer thickness. It can be seen that the Cr layer thickness has almost no effect on the equivalent wavelength of W_2 and the number of local extreme points. However, when the Cr film possesses a thickness of 15 nm, at some local extremes near the end of W_2 the curve sharpness is suppressed and there may be more uncertainties in film thickness determination. Moreover, thick Cr film indicates more light absorption, and the interference intensity will be decreased.

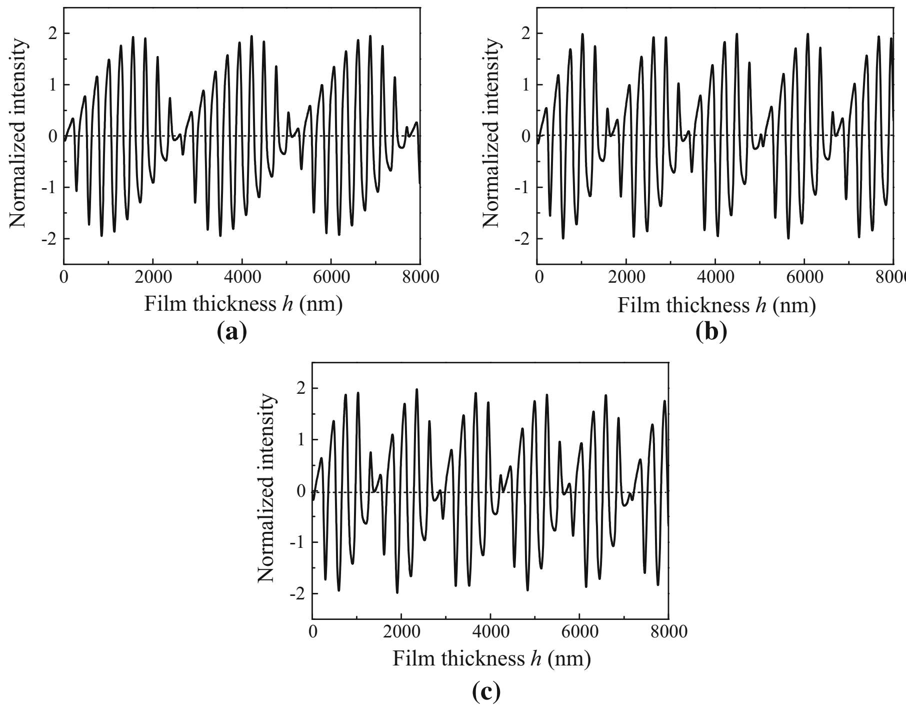

Fig. 6 I_m versus h at different red light wavelengths ($\lambda_g = 532$ nm, $h_{Cr} = 8$ nm, $n = 1.0$). **a** $\lambda_r = 593$ nm. **b** $\lambda_r = 632$ nm. **c** $\lambda_r = 653$ nm

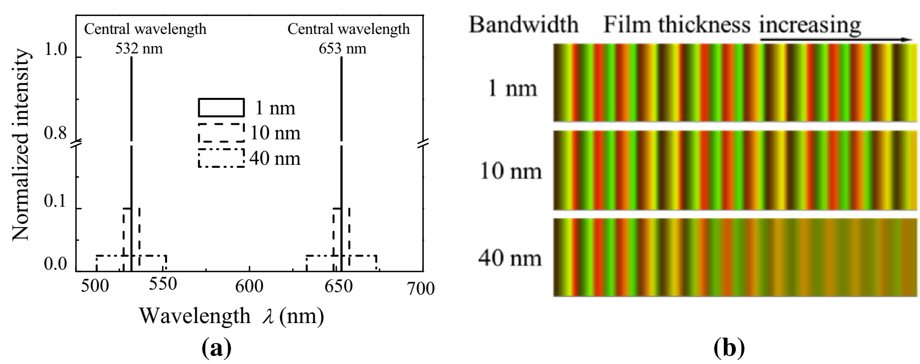

Fig. 7 Bandwidth of lights in the calculation and their influences on the fringes and colors ($\lambda_g = 532$ nm, $\lambda_r = 653$ nm, $h_{Cr} = 8$ nm, $n = 1.0$). **a** Central wavelength and bandwidth. **b** Interference fringes

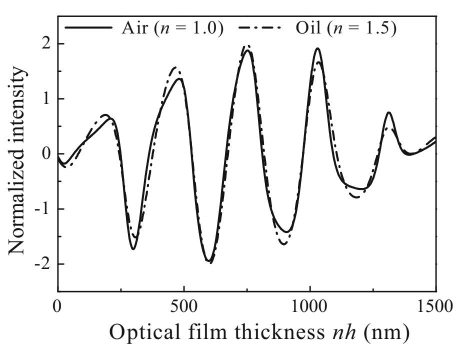

Fig. 8 Influences of lubricant refractive indices on the modulated intensity ($\lambda_g = 532$ nm, $\lambda_r = 653$ nm, $h_{Cr} = 8$ nm)

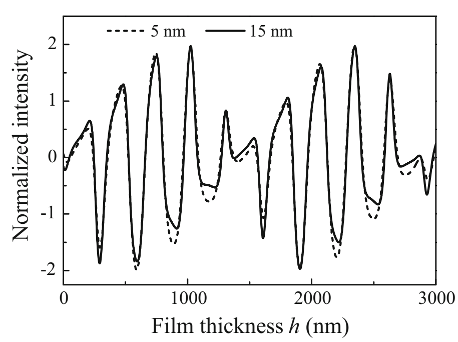

Fig. 9 Influences of Cr layer thicknesses on intensity modulation ($\lambda_g = 532$ nm, $\lambda_r = 653$ nm, $n = 1.0$)

2.3 Extension of Measurement Range

The curve of the modulated intensity signal I_m against film thickness is enveloped by the cyclic beat wave W_2 of wavelength λ_{eq}. The film thickness can be obtained at the local intensity extremes within a measurement range of $\lambda_{eq}/2$. In fact, the variation of I_m does not repeat exactly the same within every half-cycle, such that the measurement range can be extended if an individual half-circle can be identified. For the presently used dichromatic light source ($\lambda_g = 532$ nm, $\lambda_r = 653$ nm), theoretical and experimental data show that some characteristic points can be found to identify the first three half-cycles and the measurement range can be extended accordingly. As shown in Fig. 10, two characteristic points, C_{i1} and C_{i2} ($i = 1, 2, 3$) can be identified within each of the first three half-cycles. The two characteristic points C_{i1} and C_{i2} are defined in such a way that they are adjacent local extremes, $C_{i1} < C_{i2}$, and C_{i2} is the nearest to the end of a cycle. To avoid uncertainties from noise, the intensity magnitude of C_{i2} must be larger than 0.5. The criterion for identification of the half-cycle number, as extracted from the theoretical and experimental data, is given as,

$$\begin{cases} \text{1st half - cycle}: I_1 = |I_{C_{11}}| + |I_{C_{12}}| \in (1.0, 1.7) \\ \text{2nd half - cycle}: I_2 = |I_{C_{21}}| + |I_{C_{22}}| \in (1.8, 2.5) \\ \text{3rd half - cycle}: I_3 = |I_{C_{31}}| + |I_{C_{32}}| \in (2.6, 3.3) \end{cases} \quad (9)$$

Table 1 gives calculated I_1, I_2 and I_3 for the first three half-cycles with different Cr film thickness and medium refractive indices. It can be seen that the calculated results can fulfill the criterion listed in Eq. (9). Most of calculated I_1, I_2 and I_3 lie in the middle of the intervals specified in Eq. (9). Hence the specified criterion in Eq. (9) is applicable to the experiments with lubricants of different refractive indexes on a conventional optical EHL test setup.

In lubricating film measurement with DIIM approach, the interferogram under prescribed conditions is captured first and then some fringes in the interferogram are used to obtain a modulated intensity signal, for example, those out of the central contact region in an EHL contact. The modulated intensity signal can then be used to infer the film thickness at characteristic points with Eq. (9), and the fringe order for the red or green light can be obtained. After that the film thickness at any other locations, for example, the central film thickness, can be obtained by using the

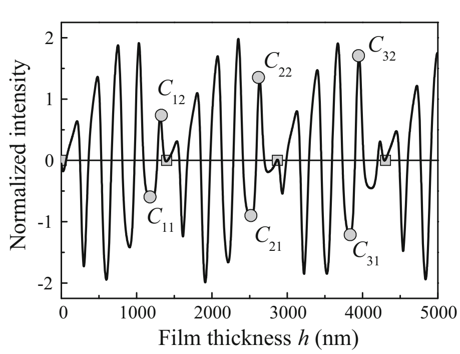

Fig. 10 Characteristic points of the first three cycles ($\lambda_g = 532$ nm, $\lambda_r = 653$ nm, $h_{Cr} = 8$ nm, $n = 1.0$)

Table 1 I_1, I_2 and I_3 under different refractive indices and Cr film thickness

	I_1	I_2	I_3
$n = 1.0$			
$h_{Cr} = 5$ nm	1.580	2.459	3.097
$h_{Cr} = 10$ nm	1.342	2.300	2.951
$h_{Cr} = 15$ nm	1.357	2.310	2.911
$h_{Cr} = 20$ nm	1.371	2.316	2.849
$h_{cr} = 8$ nm			
$n = 1.0$	1.380	2.304	2.960
$n = 1.33$	1.288	2.198	2.912
$n = 1.5$	1.273	2.162	2.894

conventional monochromatic interference intensity scheme with either the red or green light [28].

Other approaches may also be found to get the film thickness. With the modulated intensity signal, the film thicknesses at local extremes can be readily inferred after obtaining the film thickness of the characteristic point. And the film thickness at any points between two adjacent local extremes could be evaluated by their intensity. The interval between two adjacent local intensity extremes, determined by the wavelength of the carrier signal W_1, is smaller than those of the monochromatic intensity curves by λ_r or λ_g. With this small interval (wavelength), the change in film thickness leads to large variation in intensity, which benefits the resolution [19, 20]. Unfortunately, this is not true for those locations at the ends of one half-cycle because the very small intensity variation with film thickness. Another possible approach is that the beat wave, which can be obtained by some mathematical procedures with the modulated intensity curve, could be used to evaluate the film thickness. The beat wave has a wavelength larger than λ_r or λ_g and cannot achieve a high resolution. At present, the monochromatic interference intensity by λ_r or λ_g is used to measure the film thickness after the corresponding fringe order at the characteristic point is obtained. The resolution is influenced by the wavelength, the refractive index of lubricant and bit number (gray level) of the image card [19]. In the present test rig, when $\lambda_g = 532$ nm, $n = 1.5$ and 200 gray levels (30–230) from the minimum intensity to the maximum intensity (8-bit setting in the image card), an average resolution of 0.443 nm/gray level can be achieved theoretically. Taking noise signals and other factors into account, it is estimated that the thickness resolution is 1–2 nm. In fact, in the monochromatic interference approach, the resolution changes with film thickness. At the locations where intensity reaches its maximum (constructive interference) or minimum (destructive interference), the resolution is very low because the change in film thickness does not vary significantly with interference intensity. Fortunately, in the present test rig, the interference is generated simultaneously by both the red and the green lights, and the two intensities do not attain their intensity extremes at the same film thickness within the measuring range. Then a high resolution can be obtained by the duly use of the red and green intensity curves.

3 Application Examples of Film Thickness Measurements by DIIM

To test the feasibility of the DIIM approach, some case studies have been carried out under different working parameters. All the measurement given below use a dichromatic laser light with $\lambda_g = 532$ nm and $\lambda_r = 653$ nm.

3.1 Gap Measurement of a Static Hertzian Contact

The static dry contact gap between a steel ball of 25.4 mm diameter and a Cr-coated glass disk was measured with a load of 1 N. Figure 11a depicts the captured dichromatic interference image. The modulated intensity along the radial direction of the ball-on-disk contact is shown in Fig. 11b. In this static contact, the gap outside of the contact increases monotonously from zero thickness (the same in a lubricated contact), and the characteristic points in the first three half-cycles, as given in Fig. 11b, can be recognized easily. The measured $I_1 = 1.45$, $I_2 = 2.04$ and $I_3 = 2.78$ show agreement with Eq. (9). Hence, the film thickness (gap size) of one characteristic point is known and the whole gap size can thus be estimated through the intensity variation. Figure 11c shows good correlation between the measured gap and the classical Hertzian contact model. The difference between the theoretical and the experimental data at different radii is also given. The differences, which mainly come from the roughness or surface defects, are particularly small within the contact region wherein the surface roughness is flattened.

3.2 Film Thickness Measurement in a Ball-on-Disk Contact

With this DIIM approach, EHL films in a ball-on-disk were measured under pure rolling conditions. Figure 12a gives the interferograms at different speeds. The load was 10 N, and the high viscous lubricant PB1300 was chosen to

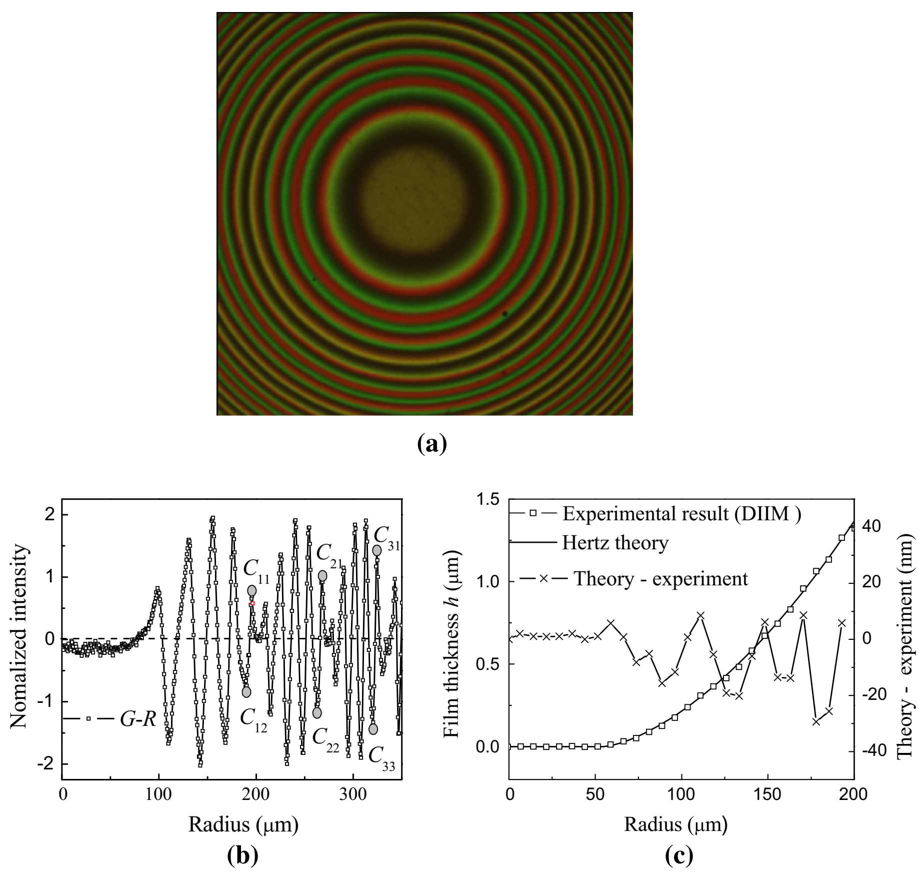

Fig. 11 Profile of the dry Hertzian contact of a static steel ball on a disk (load: 1 N, ball diameter: 25.4 mm). **a** Interference image. **b** Modulated intensity *G*–*R*. **c** Comparison of results between DIIM and theory

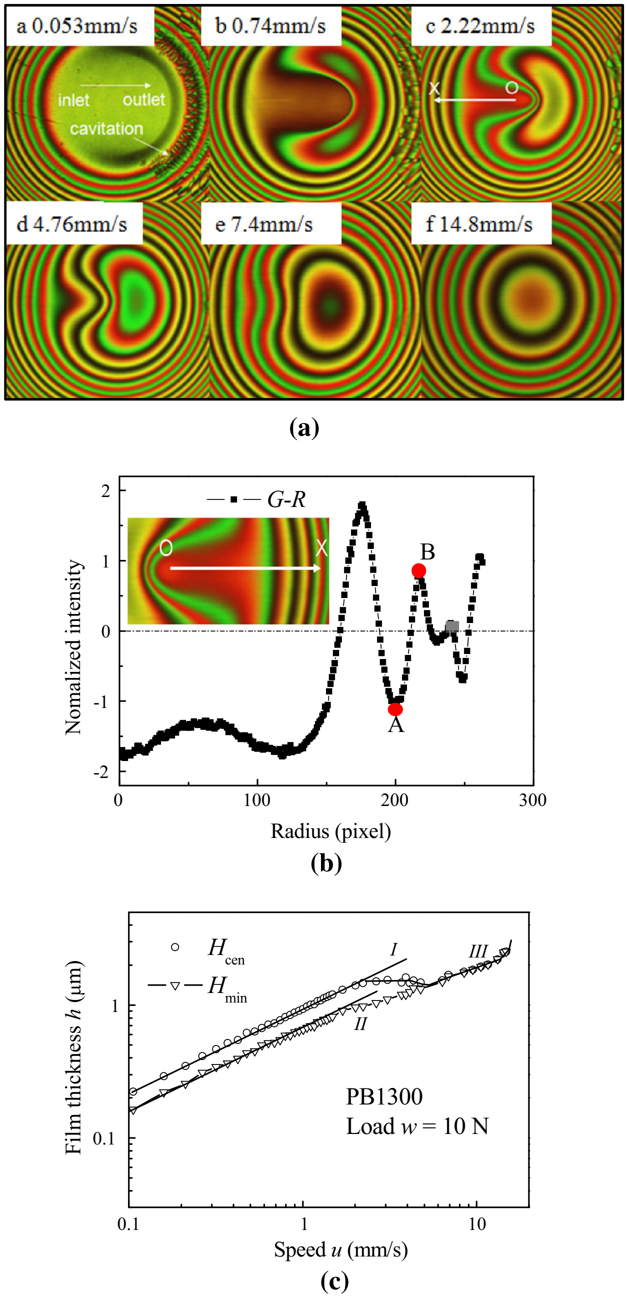

Fig. 12 Film thickness measurement in an EHL contact (lubricant: PB1300, load: 10 N). **a** Interferograms at different speeds. **b** Characteristic points and beat wave No. determination. **c** Film thickness versus speed

achieve a high film thickness. Taking the picture at 2.22 mm/s as an example, the modulated intensity curve outside the contact area is shown in Fig. 12b. It is easy to determine that the two characteristic points A and B are in the second half-circle (beat wave) from their intensity values ($|I_A| + |I_B| = 1.90$). For its film thickness, point A is between the eighth dark fringe and the eighth bright fringe according to the red light interference, and then the central film thickness and the minimum film thickness can be obtained. Figure 12c presents the measured film thickness versus speed. When the speed is less than 2 mm/s, the lubrication is in the EHL regime. The central and minimum film thickness versus speed (line *I* and *II*, respectively) holds a linear relationship at a log–log scale. The speed indices for the central film thickness and the minimum film thickness are 0.64 and 0.66, respectively, which agree with the EHL theory. When the entrainment speed increases further, the central film thickness and the minimum film thickness deviate from their original lines *I* and *II*. For further increase in speed, the two curves merge into the same line *III*. The deviations come from the recovery of the surface elastic deformation when the speed increases and the lubrication regime changes from EHL to HL, which can be seen clearly in the interferograms. It can be seen that when the speed is 14.8 mm/s, the elastic deformation totally disappears and it is naturally that the minimum film thickness occurs at the center of the contact.

3.3 Film Thickness Measurement in a Slider-on-Disk Contact

The present DIIM approach has also been incorporated into the optical slider bearing tester developed by the authors. The basic configuration of the tester is a steel slider on a Cr-coated disk contact illustrated in Fig. 13a. Details about the optical slider bearing tester can be referred to Ref. [22]. In the present experiments, three sliders of the same length of 4 mm (along the sliding direction) but different widths of 4, 6, 9 mm were used. Figure 13b gives some of the interference fringes captured, which can be used for getting modulated intensity signals. Figure 13c gives film thickness measurement results under steady conditions, in which a film thickness up to 3.75 μm is measured. In Fig. 13c, the theoretical results are also given and their correlation with the experimental results validates this DIIM approach and the test system.

The advantage of this DIIM approach was also demonstrated in the measurement of film thickness under dynamic conditions. Figure 14 illustrates the film thickness h_0 at different time instants when the disk runs with a cyclic speed as shown in Fig. 14. It can be seen that the film thickness h_0 varies with a period the same as that of the speed, and the variation range is 0.72 μm. However, the film thickness does not attain the maximum with the speed at the same instant and there is some time delay.

The limitation of the DIIM approach is that the interferogram must have enough number of fringes to cover as

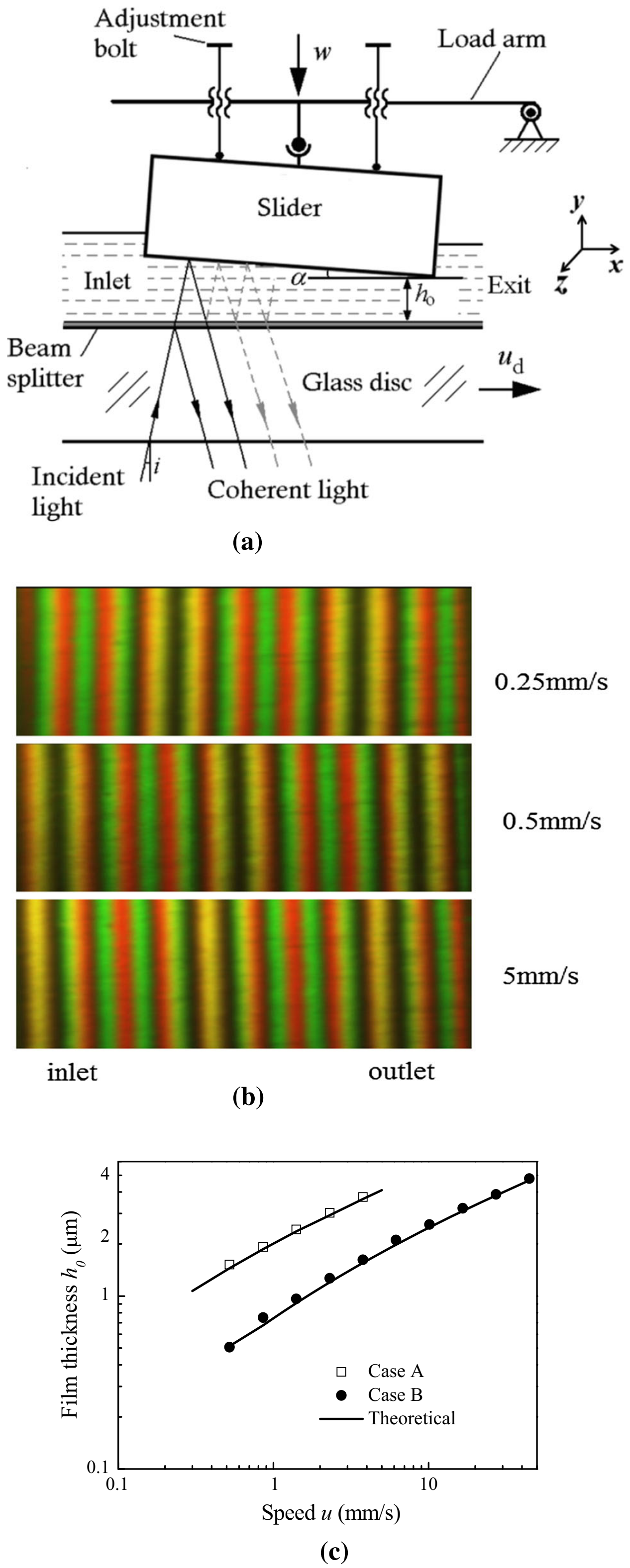

◀**Fig. 13** Film thickness measurement in a slider-on-disk contact using DIIM (Case A: PB450, load = 12 N, inclination = 5.92×10^{-4} rad, slider size = 4 × 9 mm; Case B: PAO400/40, load = 2 N, inclination = 5.40×10^{-4} rad, slider size = 4 × 6 mm). **a** An optical slider bearing tester. **b** Interferograms at different speeds, Case A. **c** Film thickness versus speed

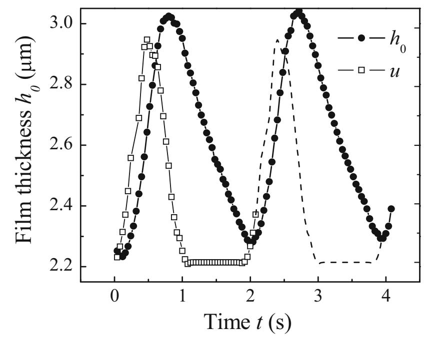

Fig. 14 Lubricating film thickness measurement in a slider-on-disk contact (PAO400/40, load = 2 N, slider size = 4 × 4 mm, inclination = 5.40×10^{-4} rad)

least the dynamic thickness range of $\lambda_{eq}/2$ in order to identify the characteristic point for reference. Hence, DIIM cannot be applied to cases of very small slider inclination or parallel plane bearings.

4 Conclusion

A DIIM approach for measuring lubricating film thickness is developed for a wide measurement range, which cannot be achieved by monochromatic interferometry due to wavelength ambiguity. Optical analyses and experiments have been carried out to clarify and validate the approach. The results are summarized as follows:

1. The dynamic measurement range of the DIIM approach was determined by the equivalent wavelength of the beat wave in the modulated intensity signal. Theoretical analyses and experiments show that the modulated intensity signal obtained from conventional optical lubrication systems is multi-beam interference dominated.
2. Application of the DIIM approach necessitates narrow bandwidths of the dichromatic light used. DIIM also requires a film thickness range up to $\lambda_{eq}/2$ to include the characteristic points at which the film thickness can be determined and serves as a reference.
3. Based on the difference in the modulated intensity signals within the first three beat wave half-cycles, characteristic points can be identified and used to extend the film thickness measurement range by three times. With the wavelengths of 653 and 532 nm on a conventional optical lubrication test setup, the measurement range is extended to 4 μm.
4. The feasibility and advantage of the DIIM approach have been demonstrated by the experiment examples.

Acknowledgments The work described in this paper was supported by the National Key Basic Research Program of China (No. 2011CB706602) and the Research Grants Council of Hong Kong (Project No. CityU123411).

References

1. Hardy, W.B., Hardy, J.K.: Note on static friction and on the lubricating properties of certain chemical substances. Phil. Mag. **38**, 32–48 (1919)
2. Kirk, M.T.: Hydrodynamic lubrication of 'perspex'. Nature **194**, 965–966 (1962)
3. Cameron, A., Gohar, R.: Theoretical and experimental studies of the oil film in lubricated point contact. Proc. R. Soc. Lond. A **291**, 520–536 (1966)
4. Foord, C.A., Hammann, W.C., Cameron, A.: Evaluation of lubricants using optical elastohydrodynamics. ASLE Trans. **11**, 31–43 (1968)
5. Gohar, R., Cameron, A.: The mapping of elastohydrodynamic contacts. ASLE Trans. **10**, 215–225 (1967)
6. Foord, C.A., Wedeven, L.D., Westlake, F.J., Cameron, A.: Optical elastohydrodynamics. Proc. Inst. Mech. Eng. **184**, 487–505 (1969)
7. Westlake, F.J.: An interferometric study of ultra thin fluid films. PhD thesis, Imperial College London, University of London (1970)
8. Wedeven, L.D.: Optical measurements in elastohydrodynamic rolling-contact bearings. PhD thesis, Imperial College London, University of London (1970)
9. Kaneta, M., Nishikawa, H., Kameishi, K., Sakai, T., Ohno, N.: Effects of elastic moduli of contact surfaces in elastohydrodynamic lubrication. ASME J. Tribol. **114**, 75–80 (1992)
10. Zhu, D., Biresaw, G., Clark, S.J., Kasun, T.J.: Elastohydrodynamic lubrication with O/W emulsion. ASME J. Tribol. **116**, 310–319 (1994)
11. Johnston, G.J., Wayte, R., Spikes, H.A.: The measurement and study of very thin lubricant films in concentrated contacts. Tribol. Trans. **34**, 187–194 (1991)
12. Glovnea, R.P., Forrest, A.K., Olver, A.V., Spikes, H.A.: Measurement of sub-nanometer lubricant films using ultra-thin film interferometry. Tribol. Lett. **15**, 217–230 (2003)
13. Cudek, V., Krupka, I., Hartl, M.: Application of spectroscopic reflectometry to elastohydrodynamic lubrication films study. Tribol. Lett. **45**, 195–205 (2012)
14. Gustafsson, L., Höglund, E., Marklund, O.: Measuring lubricant film thickness with image analysis. Proc. Inst. Mech. Eng. Part J: J. Eng. Tribol. **208**, 199–205 (1994)
15. Hartl, M., Krupka, I., Liska, M.: Differential colorimetry: tool for evaluation of chromatic interference patterns. Opt. Eng. **36**, 2384–2391 (1997)
16. Molimard, J., Querry, M., Vergne, P.: New tools for the experimental study of EHD and limit lubrications. In: Proceedings of the 25th Leeds–Lyon symposium on tribology **36**, 717–726 (1999)
17. Cann, P.M., Spikes, H.A., Hutchinson, J.: The development of a spacer layer imaging method (SLIM) for mapping elastohydrodynamic contacts. STLE Tribol. Trans. **39**, 915–921 (1996)
18. Hartl, M., Krupka, I., Poliscuk, R., Liska, M., Molimard, J., Querry, M., Vergne, P.: Thin film colorimetric interferometry. STLE Tribol. Trans. **44**, 270–276 (2001)
19. Luo, J.B., Wen, S.Z., Huang, P.: Thin film lubrication. Part I: study on the transition between EHL and thin film lubrication using a relative optical interference intensity technique. Wear **194**, 107–115 (1996)
20. Guo, F., Wong, P.L.: A multi-beam intensity-based approach for lubricant film measurements in non-conformal contacts. Proc. Inst. Mech. Eng. Part J: J. Eng. Tribol. **216**, 281–291 (2002)
21. Dalmaz, G., Chaomleffel, J.-P., Vergne, P.: An exploration of the elastohydrodynamic–hydrodynamic transition through film thickness measurements in rolling point contacts. Proc. Inst. Mech. Eng. Part J: J. Eng. Tribol. **223**, 529–540 (2009)
22. Guo, F., Wong, P.L., Fu, Z., Ma, C.: Interferometry measurement of lubricating film in slider-on-disc contacts. Tribol. Lett. **39**, 71–79 (2010)
23. Wyant, J.C.: Computerized interferometric surface measurement. Appl. Opt. **52**, 1–8 (2013)
24. Hariharan, P.: Basics of interferometry. Academic Press, New York (2010)
25. Guo, L., Wong, P.L., Guo, F., Liu, H.C.: Determination of thin hydrodynamic lubricating film thickness using dichromatic interferometry. Appl. Opt. **53**(26), 6066–6072 (2014)
26. Palik, E.D.: Handbook of optical constants of solidsII. Academic Press Inc, San Diego (1998)
27. http://www.luxpop.com/
28. Guo, F., Wong, P.L.: A wide range measuring system for thin lubricating film: from nano to micro thickness. Tribol. Lett. **17**, 521–553 (2004)